#67 dupl

Submitted to PRL 6/27/74
FERMILAB-PUB-74-162-E

#67

# Missing Mass Spectra for $p + p \rightarrow p + X$ from 9 to 300 GeV/c*

K. Abe, J. Alspector, R. Bomberowitz, K. J. Cohen, T. Delillo,
W. C. Harrison, J. Mueller, B. Robinson, F. Sannes
Rutgers University, New Brunswick, N. J. 08903

and

G. Cvijanovich and J. Oostens
Upsala College, East Orange, N. J. 07019

and

A. Colleraine
Florida State University, Tallahassee, Florida 32306

## ABSTRACT

Missing mass spectra were obtained by measuring recoil protons from the reaction $p + p \rightarrow p + X$ in the Jacobian peak region at $|t| = 0.175$ and $0.25$ $(GeV/c)^2$. The incident momentum range from 9 to 300 GeV/c was covered continuously by taking data during the acceleration ramp of the Fermi National Accelerator Laboratory machine. Our missing mass range varied from 1.5 to 8.5 GeV and we observed the well known N*(1688) and N*(2190) but no significant structures at higher mass.

*Research supported by the U. S. National Science Foundation. Development and operation of hydrogen jet target supported by the State Committee for Utilization of Atomic Energy of the U.S.S.R., Moscow.

We have searched for heavy nucleon resonances by measuring recoil protons from the reaction

$$p + p \rightarrow p + X \qquad (1)$$

in the region of the Jacobian peak. The missing mass squared is given by the expression

$$M_X^2 = m^2 - 2T_3(E_1 + m) + 2p_1p_3 \cos \theta_3 \qquad (2)$$

where m is the proton mass and the subscripts 1, 2 and 3 refer to the incident, target and recoil protons respectively. The dependence of $M_X^2$ on the incident momentum $p_1$ and the recoil momentum $p_3$ is illustrated in Fig. 1 where loci of constant $M_X^2$ are plotted at a fixed recoil angle $\theta_3 = 64.4^\circ$. For each of these loci, Jacobian peak kinematics apply where $p_1$ is a minimum for a given $M_X^2$. The value of $p_3$ for this condition to be met has little dependence on the incident momentum $p_1$. Thus by selecting a fixed angle and scanning through the entire incident momentum range during the acceleration ramp, we can take advantage of the favorable mass resolution of the Jacobian peak method without measuring $p_3$ accurately[1].

Target protons are provided by a hydrogen gas jet[2] located inside the main ring of the Fermilab machine. We detect recoil protons with a counter telescope which defines a fixed recoil angle and selects a fairly broad band of recoil momenta by means of range.

The experimental setup shown in Fig. 2 is similar to the one used in a previous experiment[3]. The major modification is the addition of three finger counters A, B and C each 0.25 in. wide which define the recoil angles more precisely and improve our resolution. Furthermore, by taking mass spectra at three different angles simultaneously any true resonance should be seen at different incident momenta. This helps discriminate against beam related effects.

The recoil proton momentum bite is determined by two aluminum absorbers by requiring the protons to go through absorber 1 and stop in absorber 2 (See Fig. 2). These events are defined by the trigger logic $C_1C_2C_3C_4C_5\overline{C}_6$. Protons are separated from pions of the same range by time-of-flight over the $\sim$2 m distance between $C_1$ and $C_4$.

In addition to proton events we record the following three triggers for monitoring the beam-target luminosity: (i) Fast charged particles passing through the spectrometer (mostly pions) are selected by means of a third absorber (see Fig. 2) with trigger logic $C_1C_2C_3C_4C_5C_6C_7$. (ii) A four fold coincidence telescope located at $70^\circ$ to the beam also detects mostly pions. (iii) A solid state detector[4] located at a fixed angle of $85.5^\circ$ to the beam measures elastically scattered protons.

The duration of the $H_2$ jet was $\sim$1 sec. whereas the full 300 GeV acceleration cycle lasts $\sim$3 sec. Therefore, our data taking was divided into three overlapping energy regions. We also took data at two different settings of $p_3$ and $\theta_3$, both at the Jacobian peak; $\theta_3 = 64.4^\circ$ and $380 < p_3 < 480$ MeV/c corresponding to an average four momentum transfer $t = -0.175$ $(\mathrm{GeV/c})^2$ and $\theta_3 = 60.0^\circ$ and $440 < p_3 < 590$ MeV/c corresponding to $t = -0.25$ $(\mathrm{GeV/c})^2$.

The incident momentum binning was chosen sufficiently fine so that its contribution to our mass resolution was small. Our mass resolution is dominated by our angular resolution which is degraded mainly by multiple Coulomb scattering. This was calculated by a Monte Carlo program giving a FWHM mass resolution $\Delta M$ of 33 MeV at $M_X = 1.6$ GeV and $\Delta M = 180$ MeV at $M_X = 7.0$ GeV for our low $|t|$ data using the finger counters. Our high $|t|$ data has $\Delta M = 22$ MeV at $M_X = 2.1$ GeV and $\Delta M = 140$ MeV at $M_X = 8$ GeV.

Fig. 3 shows a sample of our data, taken with the B finger counter, expressed in terms of the invariant cross section $s d^2\sigma/dt\, dM_X^2$. This cross section is related to the quantities measured in the laboratory by the expression

$$\frac{s d^2\sigma}{dt\ dM_X^2} = \frac{s}{2mp_1}\,\frac{\pi E_3}{p_3^2}\,\frac{d^2\sigma}{dp_3 d\Omega_3} = \frac{s}{2mp_1}\,\frac{\pi E_3}{p_3^2}\,\frac{N_P}{L\ \Delta p_3 \Delta\Omega_3} \tag{3}$$

where s is the square of the total center-of-mass energy, m is the proton mass, $N_P$ is the rate of inelastic recoil protons from Reaction (1) and L is the beam-target luminosity. The luminosity is obtained as in Ref. 5 using the rate of elastic events $N_{E\ell}$ in the solid state detector, the optical theorem, the known pp total cross section and the known pp elastic differential cross section.

The error bars ($\sim\pm1\%$) shown in Fig. 3 are statistical only. In addition, there is an uncertainty of $\pm9\%$ in the relative energy dependence of the cross section. For a more accurate measure of the energy dependence of the non-resonant cross section the reader is referred to Ref. 5. In that experiment several short jet pulses at different energies were used during a single acceleration cycle rather than a single long pulse as in the present experiment. The former method introduces fewer systematic errors in measuring energy dependence while the latter is more suitable for bump searches. Our absolute normalization was obtained by fitting the high energy part of our data to that of Ref. 5 with the error given there as ±15%.

We observe clear enhancements in the regions of the N*(1688) and N*(2190). We attempted to fit our data to compare with previous experiments[6,7] which produced these resonances in roughly the same s and t region. The suggestion is strong[6] that the cross section $d\sigma/dt$ for these and other diffractively produced N*'s is roughly s independent in the region of our data. Therefore we parameterize the bumps in our data as

$$\frac{s\, d^2\sigma}{dt\, dM_X^2}(N^*) = s\,\frac{d\sigma}{dt}\,BW(M_X) \qquad (4)$$

where $BW(M_X)$ is a suitably normalized relativistic Breit-Wigner. To this we add a background consisting of a polynomial in mass and a $1/\sqrt{s}$ term. Although the peak of the N*(1520) is below our mass range, we allow for its tail by including it in our fit with a fixed mass and width but a variable amplitude. For our highest statistics data ($t = -0.175\ (\mathrm{GeV}/c)^2$, no finger counter required) we find for the N*(1688) region M = 1675 MeV, the width with resolution removed $\Gamma = 158$ MeV and $d\sigma/dt = 1.0\ (\mathrm{mb/GeV}^2)$ in good agreement with Ref. 7. The N*(2190) region is not so well determined because the width generally wants to be wide (∿800 MeV at a mass of ∿2200 MeV).

But if we fix the width at $\Gamma$ = 300 MeV, we obtain a mass M = 2131 MeV and, in good agreement with Ref. 7, $d\sigma/dt = 0.12$ (mb/GeV$^2$). This fit includes a wide Breit-Wigner at 2350 MeV with $\Gamma$ = 1060 MeV, $d\sigma/dt = 0.24$ mb/GeV$^2$ and peak height $s d^2\sigma/dt\, dM_X^2 = 2.1$ mb/GeV$^2$. We find we need this wide bump to get a good fit (3% confidence level) although it could be interpreted as part of the background. The fit without this bump has a confidence level of less than 0.001%. Another possible interpretation is the existence of further N*'s, which cannot be resolved, above the mass of the N*(2190). Other than the N*(1688) and N*(2190), we see no evidence for bumps with widths less than 800 MeV and heights greater than $s d^2\sigma/dt\, dM_X^2$ = 2 mb/GeV$^2$.

We are grateful to the USSR-USA Collaboration (Ref. 4), in particular B. Morozov, S. L. Olsen and Y. Pilipenko, and the members of the Internal Target Laboratory for providing the hydrogen jet target facility and the elastic monitor. We also wish to thank D. Jovanovic, E. Malamud, J. Sanford and the Accelerator Section for their help and cooperation. The advice and contributions of B. Maglich and I. Siotis are warmly acknowledged.

## References


1. F. Sannes and W. C. Harrison, Nucl. Instr. and Meth. 105, 541 (1972); B. Maglich and G. Costa, Phys. Lett. 18, 185 (1965).
2. V. Bartenev et al., Advan. Cryog. Eng. 18, 460 (1973).
3. F. Sannes, T. DeLillo, M. Lieberman, J. Mueller, B. Robinson, I. Siotis, G. Cvijanovich, A. Pagnamenta and R. Stanek, Phys. Rev. Lett. 30, 766 (1973).
4. V. Bartenev, A. Kuznetsov, B. Morozov, V. Nikitin, Y. Pilipenko, V. Popov, L. Zolin, R. A. Carrigan Jr., E. Malamud, R. Yamada, R. L. Cool, K. Goulianos, I-Hung Chiang, A. C. Melissinos, D. Gross and S. L. Olsen, Phys. Rev. Lett. 31, 1088 (1973).
5. K. Abe, T. DeLillo, B. Robinson, F. Sannes, J. Carr, J. Keyne, and I. Siotis, Phys. Rev. Lett. 31, 1527 (1973).
6. J. V. Allaby et al., Nucl. Phys. B52, 316 (1973).
7. R. M. Edelstein et al., Phys. Rev. D5, 1073 (1972).

## Figure Captions

Fig. 1 Loci of constant missing masses squared at a fixed recoil angle of $64.4^{\circ}$ as a function of incident and recoil momenta. The dotted lines represent the accepted recoil momenta straddling the Jacobian peak.

Fig. 2 Experimental setup (not to scale) in the Internal Target section of the Fermilab main ring. In addition to the proton range spectrometer, there are two beam-target luminosity monitors; a solid state detector and scintillation counters BM1-4. The solid state detector is inside a vacuum chamber common to machine vacuum.

Fig. 3 Data obtained with the B finger counter in the recoil proton coincidence. The data were taken at two different angles $\theta_3 = 64.4^{\circ}$ and $60.0^{\circ}$ corresponding to $t = -0.175$ and $-0.25$ $(GeV/c)^2$ respectively. Only statistical errors of $\sim\pm1\%$ are shown. The uncertainty in the relative normalization of the data at the extremes of our energy range is ±9%. The uncertainty in the absolute normalization is ±15%.

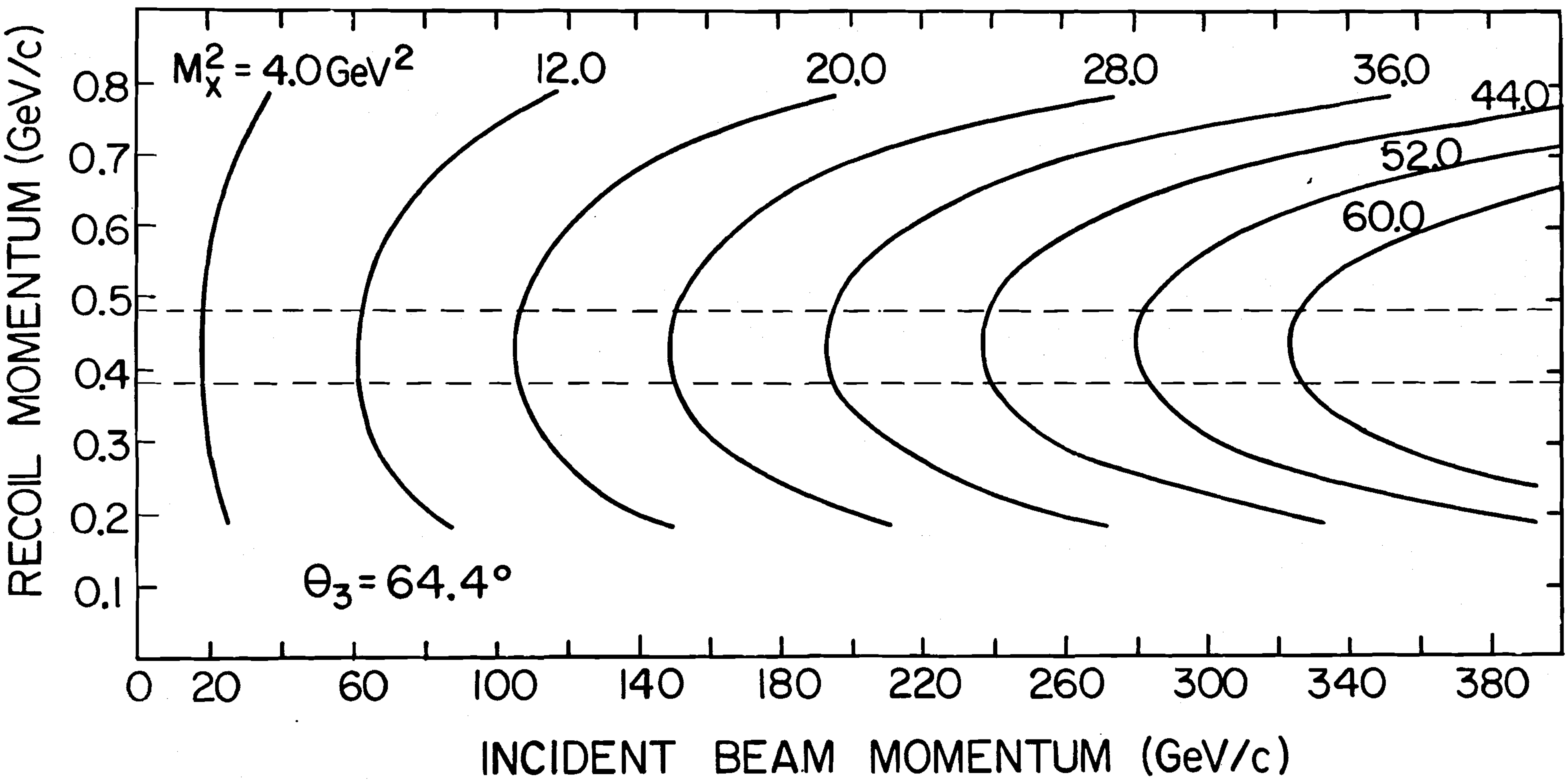

RECOIL MOMENTUM (GeV/c)
0.8
0.7
0.6
0.5
0.4
0.3
0.2
0.1
$M_X^2 = 4.0 GeV^2$
12.0
20.0
28.0
36.0
44.0
52.0
60.0
$\theta_3 = 64.4°$
0
20
60
100
140
180
220
260
300
340
380
INCIDENT BEAM MOMENTUM (GeV/c)


Fig. 1

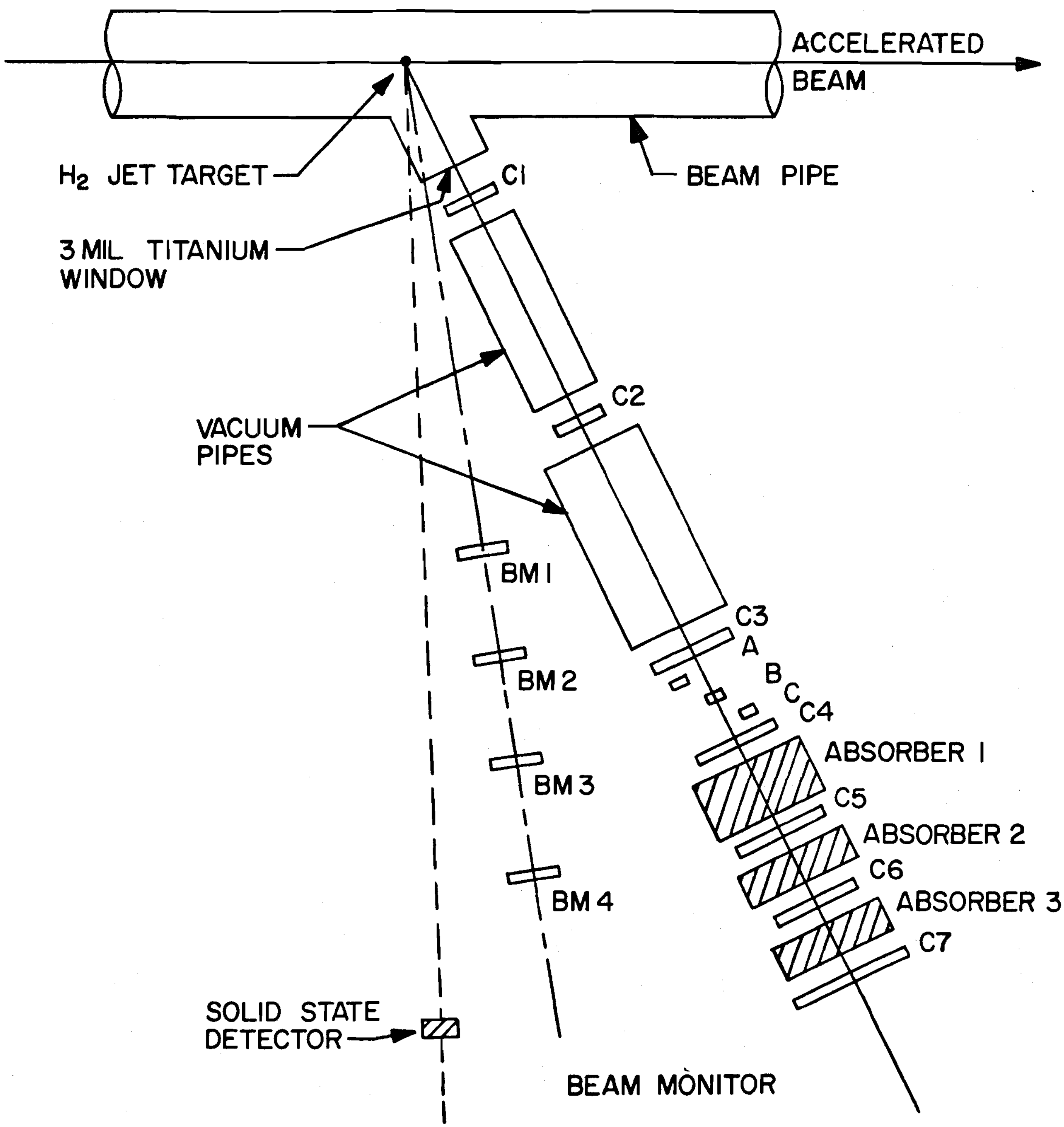

ACCELERATED BEAM
$H_2$ JET TARGET
BEAM PIPE
C1
3 MIL TITANIUM WINDOW
VACUUM PIPES
C2
BM1
C3
A
B
C
C4
BM2
ABSORBER 1
BM3
C5
ABSORBER 2
C6
BM4
ABSORBER 3
C7
SOLID STATE DETECTOR
BEAM MONITOR


Fig. 2

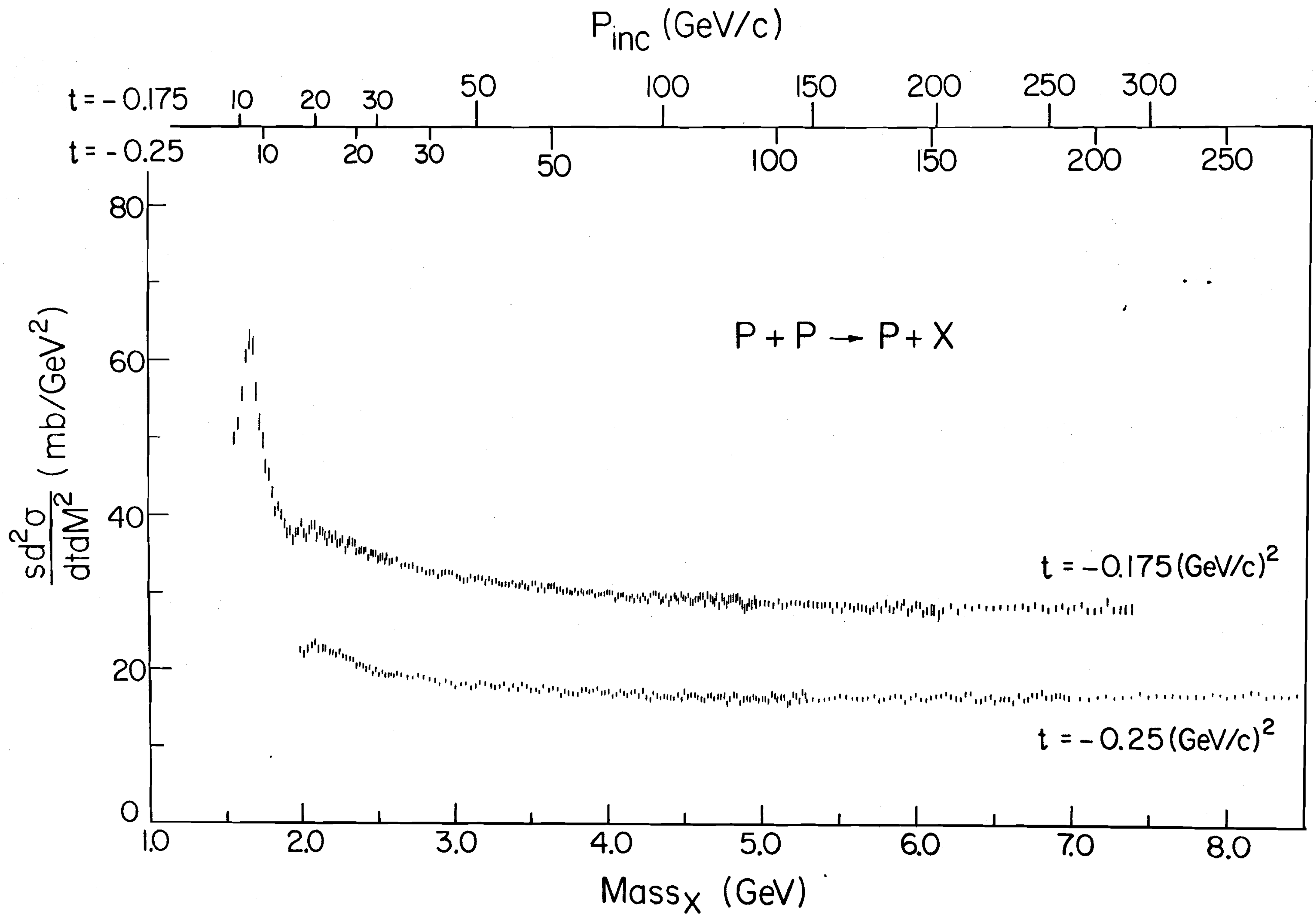

$P_{inc}$ (GeV/c)
t = -0.175
10 20 30 50 100 150 200 250 300
t = -0.25
10 20 30 50 100 150 200 250
$\frac{sd^2\sigma}{dtdM^2}$ (mb/GeV$^2$)
80
60
40
20
0
P + P → P + X
t = -0.175 (GeV/c)$^2$
t = -0.25 (GeV/c)$^2$
1.0 2.0 3.0 4.0 5.0 6.0 7.0 8.0
$Mass_X$ (GeV)


Fig. 3